Antenna Alignment and Positional Validation of a mmWave Antenna System Using 6D Coordinate Metrology

David R. Novotny†, Joshua A. Gordon, Jeffrey R. Guerrieri
Physical Measurements Laboratory
National Institute of Standards and Technology
Boulder, Colorado, United States of America
†david.novotny@nist.gov

***Abstract*— We present the positional and alignment techniques and mmWave validation for the CROMMA, an antenna measurement system that uses an industrial robot to perform probe scanning of an AUT. We improved the positional accuracy of the commercial robot by using a laser tracker to measure and correct the scanned geometry. We are measuring and positioning the probe and AUT in six degrees-of-freedom (6DoF). We combine the 6DoF position and orientation measurements (x, y, z, yaw, pitch, roll) using coordinated spatial metrology to assess the quality of each motion stage in the system, and then tie the measurements of each individual alignment together to assess scan geometry errors. Finally, we take *in-situ* 6DoF position measurements to assess the positional accuracy throughout the measurement process, which can then be used for positional error correction in the final pattern analysis.**

We performed dual polarization pattern measurements at 183 GHz. Our results show positioning errors, mmWave stability and pattern differences on two spherical scan surfaces at 100 and 1000 mm radii.

I. INTRODUCTION

The demand for millimeter Wave (mmWave) antenna measurements (> 100 GHz) has recently increased due to the practical realizations of many mmWave systems and applications. Point-to-point communication links from 92-95 GHz and 120 GHz are now commercially available and 220-650 GHz systems are being researched for medical and security applications. New developments in climate monitoring require traceability in radiometric and remote sensing equipment from 100-850 GHz, including calibrated power, emissivity and antenna gain [1].

In response to this demand, NIST has developed the Configurable Robotic Millimeter-wave Antenna Facility (CROMMA). We present here the validation testing and positional and measurement error assessment in the mmWave frequency range [2]. The CROMMA is an antenna measurement system (see fig. 1) built upon a 6 degree-of-freedom DoF robot arm used to scan a RF probe over a specified scan geometry. A 6 DoF hexapod is used to align the AUT to a ϕ-rotation stage, and a 6 DoF laser tracker (LT) used to track the 3DoF position ($\boldsymbol{x,y,z}$) and 3DoF orientation ($\boldsymbol{R_x,R_y,R_z}$ or alternatively roll, pitch and yaw) of the probe and AUT.

*US Government work, not subject to U.S. copyright.

The coordinated kinematic motion of the robot, along with its non-orthogonal motion axes, allows scanning in multiple geometries (planar, cylindrical, spherical, and linear extrapolation). Many present-day antenna ranges, including the NIST planar and spherical ranges, use dedicated stacked, orthogonal stages to generate the movement needed for a particular scan geometry. However, the orthogonality misalignments of these stages may introduce positional and/or pointing errors, which may not be fully correctable within the confines of the fixed movement stages. The use of 6DoF coordinated positioning system has been used for imaging purposes [3] and laser trackers have been used to characterize antenna ranges [4]. We are using coordinate metrology to generate 6DoF scanning geometries, and then to align multiple 6DoF movement stages and correct for the mechanical inaccuracies during the measurement. This dynamic, *in-situ* technique allows us to use less accurate but highly repeatable and configurable, positioning hardware for mmWave scanning with an eventual goal of extending the frequency range to at least 500 GHz.

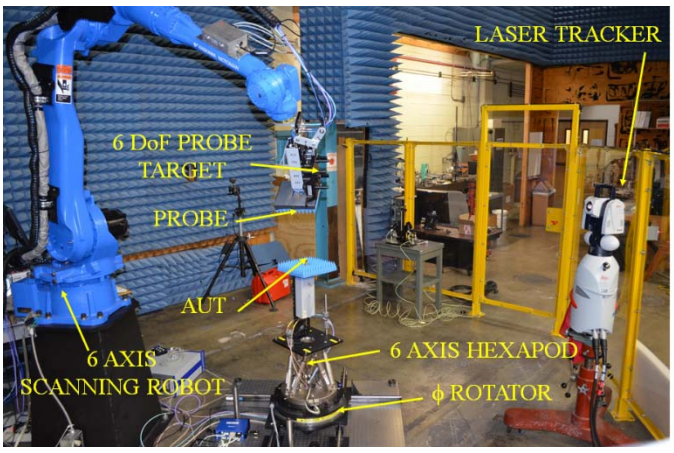

Figure 1. The CROMMA Facility. Major components include the 6-axis robot for probe scanning, the ϕ-azimuth rotator for AUT scanning, the hexapod to align the AUT to the rotator, and the laser tracker and probe targets for AUT and probe alignment and tracking.

Antenna alignment for near-field scanning was typically done at NIST with a multitude of instruments (theodolites, electronic levels, motor encoders) to align multiple stacked motion stages (linear, rotation). Many labs and systems now make use of laser trackers to measure ranges and perform periodic compensation across the scan geometry [5]. The current alignment system uses LTs with 6DoF coordinate metrology, not only for geometry creation, alignment and range qualification, but also *in-situ* positional analysis and data correction of routine measurements. This continuous position monitoring, allows for the correction of gravity, motion hysteresis, and different loading due to geometry or antenna changes. Eventually, we hope to correct for motion changes due to temperature and drive heating.

Alignment of the AUT and measurement probes to the scan geometry is often the most demanding and time consuming aspect of near-field measurements. As frequency increases, the typically acceptable positioning errors of λ/50 [6] tend to become more difficult to address. We will highlight the mechanical motion control available and the accuracies at which we can measure position of the probe and AUT.

We present pattern measurement results at 183 GHz using the CROMMA configured in an elevation over azimuth measurement coordinate system. The robot provides a $\boldsymbol{\theta}$ elevation scan over the range of -105º to 105º, while the ϕ-rotator provides 0-360º azimuth rotation.

II. Overview of the CROMMA

The CROMMA was designed around a multi-axis coordinated-motion robot. Our base requirement was to perform spherical measurements at variable distances from 50 mm to 1m in diameter, provide probe rotation for arbitrary polarizations, have the payload capacity to hold both an antenna and typical waveguide vector network analzyer (VNA) waveguide extensions, and maintain the λ/50 position accuracy up to 500 GHz. These demanding requirements dictated the need to have 6 DoF position control throughout the scanning range.

Our method to fully correct position and pointing throughout the scan does not require the alignment of multiple stages but rather the individual alignment of every scan point in the geometry. The ϕ-rotator, fig. 1, is characterized and its axis of rotation defines the system's *z*-axis. The scan geometry is arbitrary because of the full 6DoF capability of the robot. But every geometry needs to be verified by the LT. However, to get the positional accuracies similar to the axes intersection errors of other conventional dedicated geometry scanners [5], we need to use the tracker to correct for each scan geometry and probe loading of the robot.

The CROMMA has several fixed and movable coordinate systems: ϕ-rotator, hexapod, AUT, probe (ideal and measured), robot movement, alignment fixtures. These all need to be active at once and data and positional offset easily translated between multiple reference points of view. We use a commercial coordinate analysis software package that controls and coordinates the LT measurement, and keeps track of the relative position of all the components of the system.

A. Coordinate Notations

We will use the position and orientation notation of [7]. The Fixed (or extrinsic) XYZ convention for transforming between frames (compound position and rotational translations) differs from the traditional Elemental (or intrinsic) Euler Angle ZYZ convention typical of many spherical near-field antenna measurement treatises [6,8,9]. This mechanically based coordinate system is intrinsic to the robot, hexapod, and coordinate analysis software, so it is used, at least during the measurements and alignments of the system.

A frame (location and orientation) $\boldsymbol{B}$, in a Fixed XYZ coordinate system is defined by six coordinates relative to an initial frame $\boldsymbol{A}$. The Cartesian offset $\boldsymbol{x,y,z}$ from $\boldsymbol{A}$ generates the $\boldsymbol{B}$ location, and rotations $\boldsymbol{R_x,R_y,R_z}$ generate orientation relative to $\boldsymbol{A}$. Unlike traditional Euler Angle rotations, the Fixed XYZ rotations are relative to the initial fixed frame $\boldsymbol{A}$, fig, 2. There is a one-to-one mapping between the Euler ZYZ and Fixed XYZ that is used to translate the data for the final pattern analysis step.

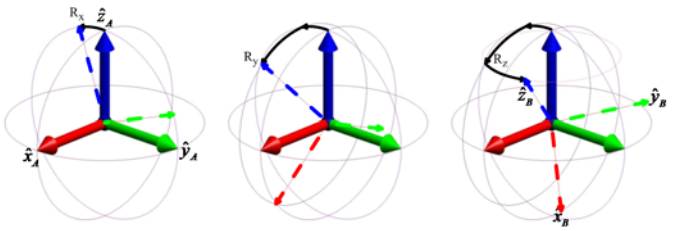

Figure 2. Rotation from Fixed XYZ frame $\boldsymbol{A}$ (solid) to frame $\boldsymbol{B}$ (dashed). The $\mathbf{R_x}$ rotation (left) about the $\boldsymbol{x}$ axis of $\boldsymbol{A}$, $\hat{x}_A$, followed by the $\mathbf{R_y}$ rotation about $\hat{y}_A$, followed by the $\mathbf{R_z}$ rotation about $\hat{z}_A$. The rotations together with the base $\boldsymbol{x,y,z}$ offset relative to $\boldsymbol{A}$, give a full 6DoF frame definition.

III. Alignment

The traditional NIST method for a spherical scan alignment for larger ranges usually requires various translation stages (roll/azimuth or elevation/azimuth) to be aligned so the axes intersect to sub-wavelength precision (typically < λ/50 or λ/25). A theodolite is placed between the AUT and probe to align the AUT and probe axes. During typical spherical alignments (2 - 40 GHz) at NIST, the imperfections in the individual axes are averaged over a rotation to minimize overall error. The AUT/probe alignments are done at one azimuth point and two opposite roll angles. The errors in probe and AUT pointing, position and drift were then limited to the movement imperfections and differential loading of the combined system. At lower frequencies these errors were considered negligible; however at mmWave frequencies, this minimization of errors could lead to larger systematic position and pointing errors at individual points in the scan

Allowable mechanical errors decrease with increasing frequency. A 300 GHz the wavelength is approximately 1 mm so typical position and pointing errors need to be less than λ/50 or ~20 μm to be able to resolve a -60 dB sidelobe [6]. At these tolerances, issues such as axes imperfections and misalignment, differential gravity loading through the scan, and repeatability of the axes become larger components of measurement uncertainty.

Rather than build a fixed circular axis for the probe scanning and accept the errors in the axis, we are using an arbitrary 6DoF robot to scan the probe. The robot was not chosen for its absolute position uncertainty (measured at ~0.4 mm) but, rather for its path repeatability (manufacturer stated rms repeatability of ~0.07 mm). If individual points can be repeated, then position errors throughout the scan can be corrected on a point-by-point basis.

The alignment and measurement processes for this system presents new challenges [10]. We will measure each movement stage to determine its base orientation, and go through repeated measure, align, re-measure to verify each sub-alignment.

A. *Base ϕ-Rotator Characterization*

The ϕ-rotator in fig. 1 is the only fixed stage of the CROMMA. We use the LT to measure the rotator movement and establish the center of the rotator and the axis of rotation, fig. 4. The AUT, probe scanning geometry, and all subsequent alignments will be referenced to the system z-axis.

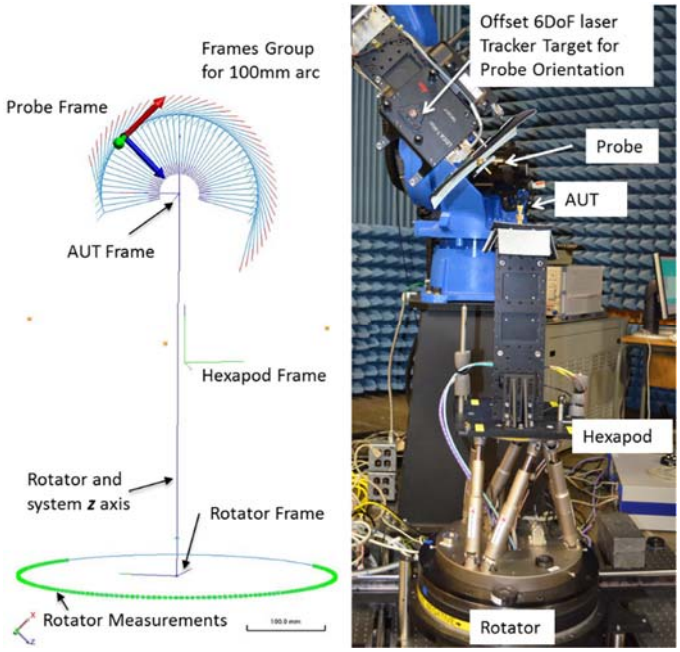

Figure 3. Alignments used in the CROMMA. The visualization of the position and orientation using the coordinate metrology software (left) is compared to the aligned hardware (right).

B. *Hexapod and AUT Alignment.*

A particular challenge at these mmWave frequencies is that the AUTs tend to be small and delicate. The size of feed horns, and the coatings on broadband reflectors do not allow for contact with LT targets or attachment of reference mirrors. NIST has developed a non-contact method of measuring the AUT and probe position and orientation, and transferring those frames to an offset 6DoF LT target [11]. The Hexapod movement frame is then measured with the LT [10]. The initial AUT position is measured and the coordinate metrology software is used to calculate the required hexapod translation to align the AUT with the system z-axis.

C. *Probe Location*

Similar to the AUT alignment, the probe frame is determined and transferred to a 6DoF target, fig 4 [11]. With the ability to measure the probe position and orientation directly, the scan geometry needs to be created. The robot is not accurately aligned to the ϕ-rotator, so an initial guess of the $\boldsymbol{\theta}$ elevation scan will lead to position and pointing errors that need to be addressed, figs. 4 - 5.

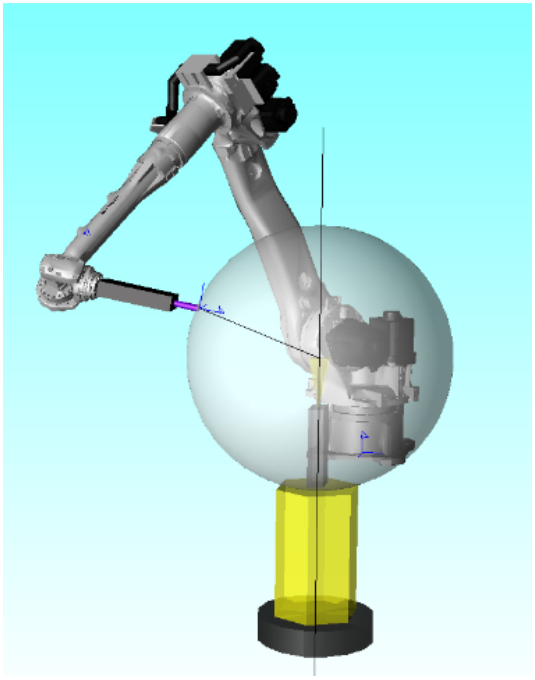

Figure 4. Conceptual image of pointing errors in the CROMMA. The sphere represents the ideal scan geometry and the line between the probe and the scan center highlights a correct probe position and incorrect probe pointing. Both types of errors are correctable in the CROMMA.

The initial scan will show the base robot error and misalignment. This is due mainly to robot alignment uncertainty and the gravity loading of the robot as the probe is scanned through the scan geometry. The resultant difference between the ideal and the measured probe frame, fig. 5, is determined by the coordinate metrology software and it calculates the correction in the robot movement frame for every scan point. This updated robot scan geometry is uploaded for re-verification by the LT.

The six-axis structure of the robot requires multiple axes to move between any two arbitrary probe locations, so single axis corrections are not sufficient for accurate probe positioning and orientation. The robot's overall accuracy was measured at ~400 µm; its measured repeatability, ~20 - 50 µm, is considerably better. Because local robot movement frames vary slightly due to gravity, loading, and robot imperfections, to get overall accuracies on the order of the base robot repeatability, multiple corrections to the path need to be performed using multiple axes to overcome the local irregularities in the robot movement.

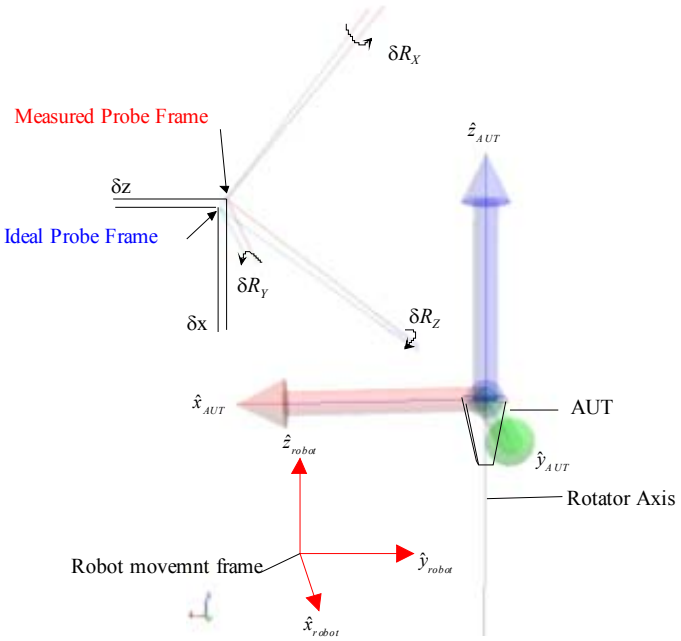

Figure 5. Position correction using multiple frames. The ideal and measured probe frames are defined relative to the AUT frame. The corrections (δx, δy, δz, δRx, δRY, δRZ) are calculated in the robot's absolute movement frame and sent as corrections to the robot trajectory. Note that for this case, the ideal probe location (***x,y,z,R*****x****,R*****y****,R*****z***) or (79.86 mm, 0 mm, 60.12 mm, 180º,53º,180º) corresponds to an Euler (***r, θ, ϕ, χ***) of (100 mm,53º,0º,0º) and pointing at the AUT origin.

We setup an elevation-over-azimuth spherical measurement at a radius ***r*** =100 mm with a ***θ*** elevation scan from −105º to 105º. We set the scan center at the AUT aperture and set ϕ=0º and the polarization χ =0º. The ***θ*** scan was run in both the forward and reverse directions to correct for differential path inaccuracies due to direction. The results, figs. 6-7, show that mean position errors are correctable to 25 µm and the pointing errors are reduced to less than 0.02º with three iterations.

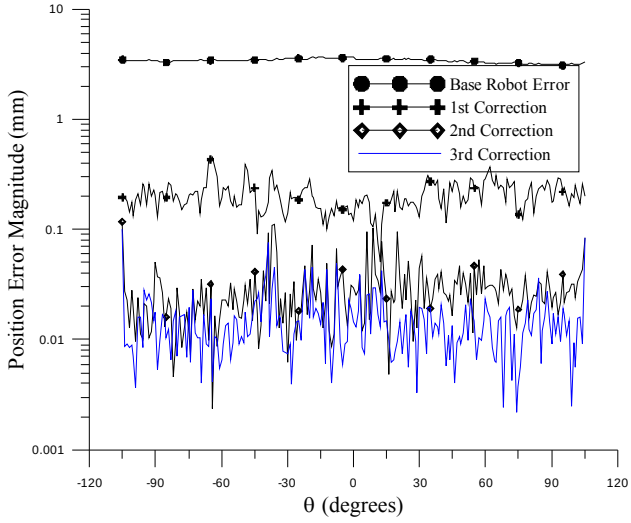

Figure 6. Scan geometry correction as a function of scan position and correction iteration. Some residual errors are seen around -32º and +5º which can be correctable with a nonlinear correction algorithm.

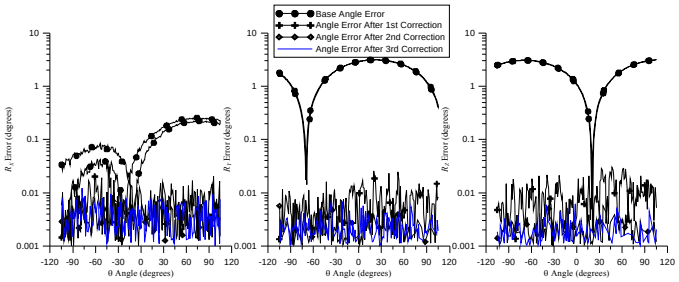

Figure 7. Pointing angle correction as a function of scan position and correction iteration. 6DoF target uncertainty is specified at ~0.01º. The base path has a forward to reverse difference seen in the ***R*****X** pointing angle (left), this is addressed by the point-wise geometry correction.

IV. REPEATABILITY

The long-term repeatability of the CROMAA was assessed by comparing the probe frame variations during a series of twenty ***θ*** scans (25 minutes) to a full 360º ϕ scan (14 hours). 6DoF position as well as mmWave insertion at 183 GHz were recorded. Fig. 8 shows the range of robot movment required to perfrom a 100 mm radius spherical scan. The movement of the micrwave cabling needs to be miminized to prevent signal drift.

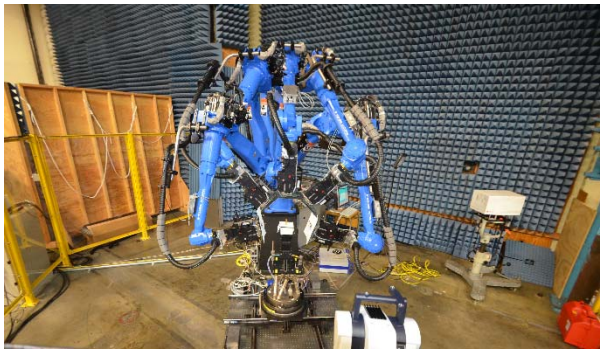

Figure 8. Robot and mmWave hardware movement during a −105º to +105º ***θ*** scan.

A. Position Repeatability

The short-time twenty scan data, fig. 9, shows a measured radius of 99.998 ± 0.016 mm. The full scan, fig. 10, shows a radius of 99.976 ± 0.022 mm. The average radius seems to shrink by approximately 20 µm as the measurement proceeds, fig 11. This is primarily due to the thermal changes in the robot as the robot comes to a different quiescent operating point than during the alignment process. After the measurement is over and the robot has an opportunity to thermally stabilize again, the robot returns to the base profile measured in fig 9. While this raises concerns at higher frequencies (>300 GHz), the amount of change, approximately 20 µm, still results in an overall uncertainty of less than λ/50 or 32 µm at 183 GHz. The ability to capture full 6DoF scan data throughout the scan will, in the future, allow for either *in-situ* measurement correction of path or post-measurement, full-6DoF correction of the mmWave data to the actual measured positions.

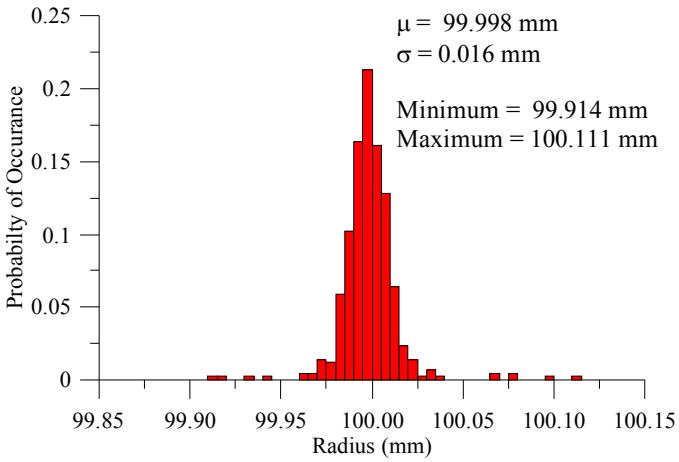

Figure 9. Radius histogram of twenty scans. The average radius is within the laser tracker uncertainty (10 µm) of the target 100 mm. The position uncertainty of 16 µm is less the λ/50 error, 32 µm, for discrimination of a -60 dB sidelobe at 183 GHz.

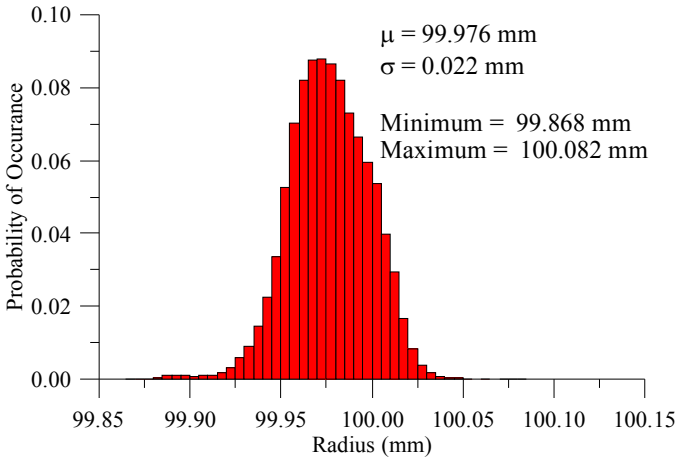

Figure 10. Radial uncertainty for the full 14 hour measurement. The uncertainty has grown to 22 µm.

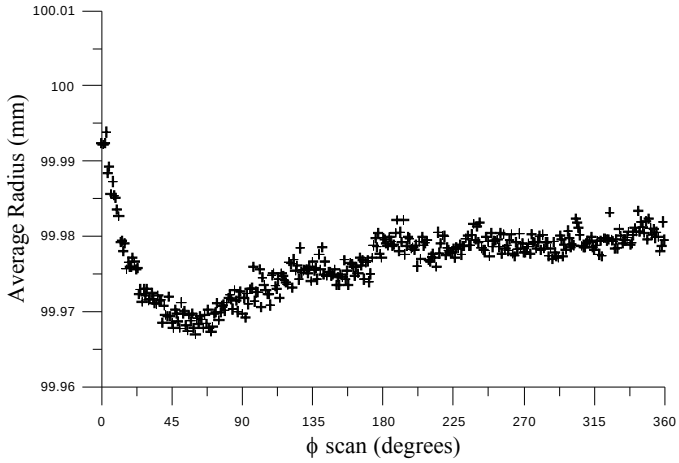

Figure 11. Mean radius as a function of ϕ position, or time. As the robot warms during long operations, the positional calibration changes slightly and introduces an ~20 µm position shift. This can be accounted for in future efforts at higher frequencies by pre-compensating the path for this effect, *in-situ* path correction, or post-processing the mmWave data to account for the positioning error.

B. mmWave Repeatability

The stability of the position data allows us to measure the mmWave data with minimal concern that the variations in data are due to robot positioning errors. Amplitude and phase drift due to cable movement and thermal drift has to be analyzed to determine if it introduces significant effects on the measured pattern. Other research has raised concerns that use of externally driven sources and mixers [12] over moderate (1 m) distances may introduce unwanted errors. An advantage of the use of an industrial motion stage designed for tens of millions of operations is that cable routing is specifically designed for minimal cable stress. This is very useful for avoiding stress on microwave cabling. Fig. 12, shows the twenty scan mmWave data at zenith (θ=0º, ϕ=0º). The amplitude (< ±0.03 dB) and phase repeatability (< ±7º) are within established norms for near-field scanning measurements [6].

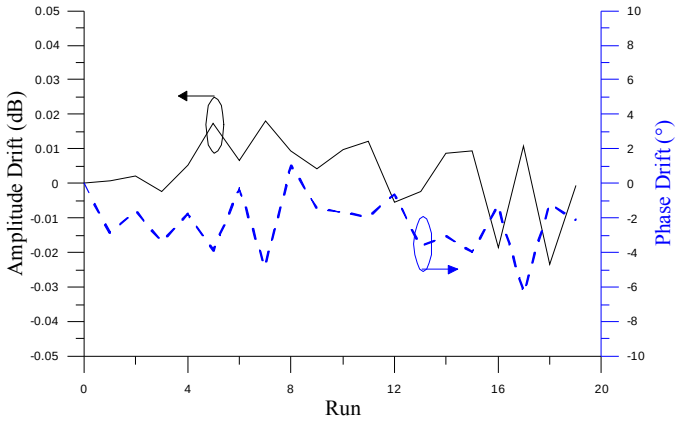

Figure 12. Zenith mmWave repeatability data for twenty θ = +105º to -105º scans. The microwave cables feeding the mmWave hardware undergo a displacement >100 cm while maintaining ±0.03 dB and ±7º stability at 183 GHz.

V. Pattern Data

The elevation over azimuth data were performed at two polarizations and at two radial distances of 100 mm and 1000 mm. This required four path calibrations: $\chi = 0^{\circ}$ and 90° at both 100 and 1000 mm. The far-field patterns, fig. 13, derived from the 100 and 1000 mm scans for both the E- and H-planes agreed to within ±0.5 dB above the -20 dB pattern level [13].

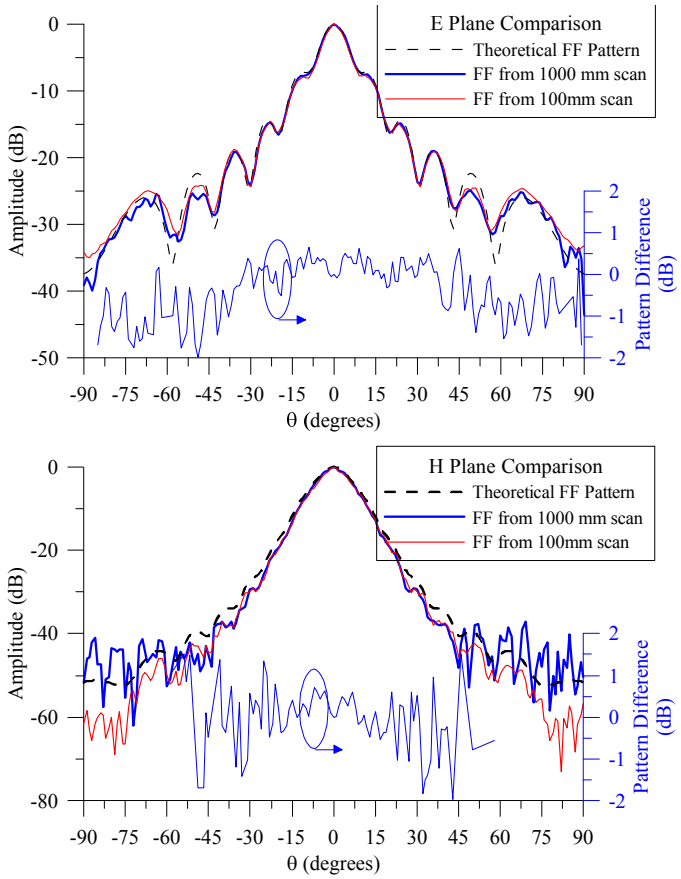

Figure 13. Theoretical, measured E-Plane (top) and H-Plane (bottom) patterns from two radial distances. The difference between the 100 and 1000 mm scan data is within ±0.5 dB for the central peak.

We can see, especially in the 1000 mm scan data that the noise floor is reached at large $\boldsymbol{\theta}$ angles. This may be a future issue when measuring large antennas at high frequencies when very low-level side-lobe (<-50 dB) information are needed. This might be addressed by reducing the scan speed and increasing dwell time at each measurement point (at the cost of increased measurement time) or additional system gain (increased cost).

VI. Conclusions

We have shown that using a 6DoF probe scanning and positional measurement hardware can provide adequate positioning for measuring patterns at 183 GHz. We are using a commercial material handling robot guided by metrology grade LTs and coordinate measurement software to perform near-field scanning with the precision required up to 300 GHz. The full 6DoF positioning, measurement and corrections performed allow for variable scanning, such as spherical, cylindrical, planar and extrapolation geometries. The 6DoF information also allows for mechanical position correction and post-measurement software correction of the collected data. We can use minimally accurate, but highly repeatable, lower-cost motion stages to deliver performance that may be cost prohibitive in custom single-axis motion systems.

We hope to be able to extend the frequency range in the future by bringing online algorithms that use the actual, non-ideal measurement locations measured by the LT [6]. We are currently correcting the scan geometry for the gross robot alignment, kinematic model and gravity loading effects to within ±25 µm. We will be addressing the robot dynamic and thermal changes that happen during long operational periods.

References

[1] D.A Houtz, D. Gu, D.Walker, J. Randa, "An Investigation of Antenna Characterization Techniques in Microwave Remote Sensing Calibrations," IEEE International Geoscience and Remote Sensing Symposium, Munich, July 2012.

[2] J.A. Gordon, D.R. Novotny, M.F. Francis, R.C. Wittmann, "The CROMMA Facility at NIST Boulder: A Unified Coordinated Metrology Space for Millimeter-Wave Antenna Characterization," 2014 Proceedings of the Antenna Measurement Techniques Association.

[3] N. Petrovic, T. Gunnarsson, N. Joachimowicz, M. Otterskog, "Robot controlled data acquisition system for microwave imaging," 3rd European Conference on Antennas and Propagation (EuCAP), pp. 3356 – 3360, 2009.

[4] G. Hindman, A. Newell, L. Dicecca, J.C. Angevain, "Alignment Sensitivity and Correction Methods for Millimeter-Wave Spherical Near-Field Measurements," 2010 Proceedings of the Antenna Measurement Techniques Association, pp. 316–321, 2010.

[5] J. Fordham, T. Schwartz, G. Cawthon, Y. Netzov, S. McBride, M. Awadalla, D. Wayne, "A Highly Accurate Spheriecal Near-Field Arch Positioning System," AMTA 2011, pp. , Oct. 2011.

[6] R.C. Wittmann, B.K. Alpert, M.H. Francis, "Spherical near field antenna measurements using non-ideal measurement locations," 2002 Proceedings of the Antenna Measurement Techniques Association, pp 43-48, October 2002.

[7] J. J. Craig, Introduction to Robotics: Mechanics and Control, 3rd ed. New Jersey, Prentice Hall, 2004, pp. 38-74.

[8] A.C. Ludwig, "Near-Field Far-Field Transformations Using Sphereical Wave Expansions", IEEE Trans. A&P, March 1971, pp 214-220.

[9] J.E. Hansen, Sphereical Near-Field Antenna Measurements, Exeter, Peter Peregrinus, 1988.

[10] D.R. Novotny, J. Gordon, J. Coder, J. Guerrieri, M. Francis, " Use of a Laser Tracker to Actively Coordinate the Motion of a 3-meter Industrial Robot to Within 50 Microns," Journal of the CMSC, Autumn 2013, Vol 8, No 2, pp 26-32.

[11] J.A. Gordon, D.R. Novotny, "A Non-Contact Machine Vision System for the Precision Alignment of mm-Wave Antennas in all Six Degrees of Freedom," 2014 Proceedings of the Antenna Measurement Techniques Association.

[12] M. Htizler, S. Bader, C. Waldschmidt, "Key aspects of robot based antenna measurements at millimeter wave frequencies," 8th European Conference on Antennas and Propagation (EuCAP), pp. 474-478, 2014.

[13] M.H. Francis, R.C. Wittmann, D.R. Novotny, J.A. Gordon, "Spherical Near-Field Measurement Results at Millimeter-Wave Frequencies Using Robotic Positioning," 2014 Proceedings of the Antenna Measurement Techniques Association.